Title	Time-Variant Simulation of Multi-Material Thermal Pultrusion
Author(s)	Joshi, Sunil Chandrakant; Chen, X.
Citation	Joshi, S. C., & Chen, X. (2011). Time-Variant Simulation of Multi-Material Thermal Pultrusion. Applied Composite Materials, 18(4), 283-296.
Date	2010
URL	http://hdl.handle.net/10220/39015
Rights	© 2010 Springer Science+Business Media B.V. This is the author created version of a work that has been peer reviewed and accepted for publication by Applied Composite Materials, Springer Science+Business Media B.V. It incorporates referee's comments but changes resulting from the publishing process, such as copyediting, structural formatting, may not be reflected in this document. The published version is available at: [http://dx.doi.org/10.1007/s10443-010-9156-9].

TIME-VARIANT SIMULATION OF MULTI-MATERIAL THERMAL PULTRUSION

S. C. Joshi and X. Chen
School of Mechanical and Aerospace Engineering
Nanyang Technological University, Singapore 639798

E-mail: mscjoshi@ntu.edu.sg

Abstract

Pultrusion being the viable and economical process for producing constant cross-section composite products, many variants of it are being tried out. This paper embarks on the pultrusion with multi-materials; typically foam/FRP sandwich panels. Unlike conventional composites pultrusion, this process with more than two material phases, one of them dry, poses a challenge in simulating the thermal co-curing within the die. In this paper, the formulation and development of three-dimensional, finite element/nodal control volume (FE/NCV) approach for such multi-material pultrusion is presented. The numerical features for handling the dry-wet material interfaces, material shrinkage, variations in pull speed and die heating, and foam-to-skin thickness ratio are discussed. Implementation of the FE/NCV procedure and its application in analyzing pultrusion of polymer foam/ GFRP sandwich panels with multi-heater environment are presented.

Keywords: A: foam sandwich; B: Curing; C: Finite element analysis; E: Pultrusion

1. Introduction

The pultrusion process involves passing of resin-impregnated fibres or other preforms continuously at certain speed through a die for shaping as well as gradual curing the composite part. The die entrance is generally characterized by a tapered shape to remove the excess resin and sufficiently consolidate the material. The pultrusion process works well with quick-curing resins and is a very low-cost method for high-production of parts with constant cross-sections [1].

The interest in developing numerical models for simulation of complex manufacturing processes is well recognized [2]. In particular, the importance of heat transfer and cure analysis in pultrusion has been identified long ago for obtaining a product with desired mechanical properties [2-5]. Chachad et al. [6] proposed a three dimensional model of heat transfer and cure for pultruded materials. Suratno et al. [7] proposed a coupled procedure for modeling three-dimensional (3D) heat transfer and cure using a general-purpose FE software. A group of researchers [8-10] investigated thermochemical aspects of the process and developed numerical models and implemented them using finite element/ nodal control volume (FE/ NCV) techniques. The temperature dependent material properties and resin shrinkage were taken into account by Joshi et al., who in [9-10] proposed an optimization procedure based on the FE/ NCV technique. Li et al. [11] carried out experimental and theoretical analysis of pulling force in pultrusion, in which the composite separation points from the die wall were predicted using resistance force model. Carlone et al. [12-13] employed finite difference method to simulate pultrusion process and subsequently proposed a hybrid method, e.g. simplex approach and genetic algorithm, to optimize accuracy of the manufacturing. A micromechanics based 3D framework was proposed for the nonlinear analysis of pultruded fiber-reinforced polymeric composites using a nested multi-scale approach and homogenization technique [14]. A multi-

scale modeling framework is recently proposed for generating the effective nonlinear thermo-viscoelastic responses of multi-layered and thick-section composites by Muliana and Haj-Ali [15]. Several experimental investigations on pultrusion were performed by Batch and Macosko [16] and Britnell et al. [17].

Despite these numerical and experimental investigations on pultrusion process, only few [18-19] attended to pultrusion of foam sandwich panels, which are sought in for building railway carriages and carrier trucks. On the contrary to the pultrusion of monolithic composites, process simulation of sandwich composites pultrusion poses many challenges. The simultaneous movement of dry, solid and non-curable foam within the die along with wet, compactable and curable resin-fibre mix on both sides of the foam results in dry-wet as well as porous-non porous surface contacts. With the rising temperatures, these two materials experience differential shrinkage. The different thermal conductivity of these two materials also affects the curing process for the face-sheets. Thus, certain specific features and numerical treatment is required for the process simulation.

Three dimensional modelling of pultrusion of foam sandwich panels, which takes into account thermo-chemical aspects of the process, is analyzed in this paper. The model considers heat transfer, mass transport and related convective effects, exothermic heat of resin cure reaction, and material shrinkage. The various coupled as well as decoupled numerical schemes developed are presented. Special issues pertinent to the manufacturing of multi-material sandwich panels are discussed. Simulation case studies on the pultrusion of polymer foam/ GFRP sandwich panels with multi-heater environment demonstrating the application of the 3D FE/NCV procedure are presented.

2. Thermoanalysis of pultrusion

2.1. Heat transfer within die assembly

The modelling of pultrusion begins with heat transfer within the entire die assembly shown in Fig. 1(a). Different energy balance equations of the forming die and the composite materials are required, taking into account the exothermic resin cure reaction and convective effect, related to the movement of the processing part [20]. In 3D Cartesian coordinate system with z axis as the pull direction, the energy balance for die (denoted by subscript *d*), fibre-resin composite face sheets (denoted by subscript *c*) and polymer foam (defined by subscript *fo*) can be written respectively as equations (1) to (3) below:

$$\rho_d c_{p,d}\left(\frac{\partial T}{\partial t}+\frac{\partial\left(v_z T\right)}{\partial z}\right)=\nabla\left(k_d \nabla T\right) \tag{1}$$

$$\rho_c c_{p,c}\left(\frac{\partial T}{\partial t}+\frac{\partial\left(v_z T\right)}{\partial z}\right)=\nabla\left(k_c \nabla T\right)+\rho_r \phi_r H_r \dot{R}_r\left(\alpha\right) \tag{2}$$

$$\rho_{fo} c_{p,fo}\left(\frac{\partial T}{\partial t}+\frac{\partial\left(v_z T\right)}{\partial z}\right)=\nabla\left(k_{fo} \nabla T\right) \tag{3}$$

where ρ is the die material density, c_p the specific heat, and k the thermal conductivity. Depending upon the nature of the material (isotropic or orthotropic) conductivity in x, y and z direction can be defined. ϕ_r represents the resin volume fraction ($\phi_r = 1-\phi_f$; ϕ_f being the fiber volume fraction), v_z the pull speed, H_r the total heat of reaction per unit mass of resin, and the subscript *r* denotes the matrix (resin).

2.2. Composites cure kinetics

During pultrusion process when the composites mass containing a reactive resin moves through a forming die, the exothermic cure reaction causes increase in material temperature [12]. The associated conservation of chemical species during the reaction can be expressed as [20]:

$$\dot{R}_r(\alpha) = K_0 \exp\left(\frac{-\Delta E}{RT}\right)(1-\alpha)^n + v_z \frac{\partial \alpha}{\partial z} \tag{4}$$

where $\dot{R}_r(\alpha)$ is the rate of resin reaction, $\alpha = \alpha(t)$ the degree of cure (conversion fraction of the reactive species that varies from 0 to 1 for uncured and full cured resins, respectively), referred in this paper as DOC for convenience, and t the reaction time. The K_0 is a constant, E the activation energy, T the absolute temperature, R the universal gas constant, n the order of the reaction (kinetic exponent). H_r and $\dot{R}_r$ can be fitted to a model experimentally using differential scanning calorimetry (DSC) measurements.

3. Time variant process simulation

3.1 FE/ NCV scheme

Field theory deals with physical situations characterized by the Laplace's equation or its variants that describe the laws of gravitational or magnetic force, conductive heat transfer, electric current flow, fluid flow through permeable media etc. Many commercial FE packages contain a field analysis module because of its versatility in application. For example, Eq. (5) below is solved for transient thermal conduction analysis in LUSAS [21]:

$$\rho C_p(\varphi)\frac{\partial \varphi}{\partial t} = \nabla\left[S_i(\varphi)\nabla\varphi\right] + H(\varphi) \tag{5}$$

where, φ, $S_i(\varphi)$ and $H(\varphi)$ represent T, k and $\frac{\partial H}{\partial t}$ respectively.

The pultrusion process is characterized by the non-linearity related to the coupling between the energy Eqs. (1)-(3) and the species Eq. (4). As a result, even with constant material properties, the finite element matrix with the nonlinear and coupling characteristics becomes too difficult to be solved by several commercial finite element packages. The LUSAS finite element code, used for the present investigation, allows solving non-linear problems. However, taking into account that the rate of cure reaction is a function of the temperature and the temperature field can be strongly influenced by the generative term due to the exothermic reaction, direct implementation of the generative term into the FE analysis is not possible.

An approach based on a finite-element/nodal-control-volume (FE/ NCV) technique, has been therefore proposed using both, the finite element and the finite difference methods [6, 8-9]. The finite difference grids and the nodal control volumes are constructed onto the finite element mesh. A schematic of a typical FE/NCV discretization of a pultrusion die-composite assembly for sandwich structure is shown in Fig. 1(b). The convective and the generative terms are decoupled from the energy equation and evaluated at the previous time step [9]. Thus, a relatively simpler and more accurate computational procedure is proposed in this paper. Taking into account the imposed boundary conditions, the steady state temperature field is initially calculated, assuming the degree of cure as null and the composite temperature as the temperature of the resin bath at each node. At the each representative point in the composite material, the degree of cure is obtained using Eq. (4) at a semi-steady state condition over the small pre-defined time step [9].

Before inducing the solution algorithm, boundary conditions are assigned to the model to define realistic process parameters and to meet the requirements of this particular heat transfer problem.

A constant temperature is applied at the walls. The thermal symmetry conditions generally involve a zero temperature gradient in normal direction, which is equivalent to adiabatic sealed boundaries. Fig. 1(c) shows all the relevant boundary conditions applied in the simulation. The interface between the part and the die is modeled as a thermal contact surface [21]. The constantly moving composites of fibre bundles, polymer matrix and foam are assigned with a uniform pulling velocity. The microscopic flow velocities within the composites are neglected since the macroscopic movement of the composites within the die is dominating the problem. All other degrees of freedom in the domain remain free and are to be determined by the solver.

In this approach, the domain of interest is sub-divided first into a number of finite elements for performing heat transfer analysis. Three-dimensional heat transfer in a continuously moving composite preform in a pultrusion die at speed v_z, is modelled to obtain the nodal temperatures respectively for die, composites, and foam using:

$$\rho_d C_{p,d}\left[\frac{\partial T}{\partial t}\right]^{k+1} = \left[\nabla\left(k_d \nabla T\right)\right]^{k+1} \tag{6}$$

$$\rho_c C_{p,c}\left[\frac{\partial T}{\partial t}\right]^{k+1} = \left[\nabla\left(k_c \nabla T\right)\right]^{k+1} + \underbrace{\left[\frac{\partial H}{\partial t}\right]^{k} - \rho_c C_{p,c}\left[\frac{\partial\left(v_z T\right)}{\partial z}\right]^{k}}_{H_c(t)} \tag{7}$$

$$\rho_{fo} C_{p,fo}\left[\frac{\partial T}{\partial t}\right]^{k+1} = \left[\nabla\left(k_{fo} \nabla T\right)\right]^{k+1} - \underbrace{\rho_{fo} C_{p,fo}\left[\frac{\partial\left(v_z T\right)}{\partial z}\right]^{k}}_{H_{fo}(t)} \tag{8}$$

NCVs are generated around the FE nodes, as shown in Fig. 1(b). The convective term in Eqs. (7) and (8) at time step k is obtained at the previous time step. H_c(t) in Eq. (7) supplied as the source term at the nodes bound by the respective NCVs can be determined using the previous

DOC. Using the proposed scheme, the convective and exothermic terms in Eq. (7) can be decoupled from the rest of energy equation. Because of the decoupling, the exothermic term for the reactive component, $\left[\frac{dH}{dt}\right]^k$, can be easily set as zero for the foam elements. For the GFRP elements, the $\left[\frac{dH}{dt}\right]^k$ term is calculated as below:

$$\left[\frac{dH}{dt}\right]^k = H_r\left[K_0 \exp\left(\frac{-\Delta E}{RT}\right)(1-\alpha_t)^n + \frac{\partial(v_z \alpha_t)}{\partial z}\right]^k \tag{9}$$

$$\alpha_t^k = 1 - \left[1 + (1-n)S^k\right]^{\frac{1}{1-n}} \tag{10}$$

$$S^k = K_0 \exp\left(\frac{-\Delta E}{RT^k}\right)\left(t^k\right) \tag{11}$$

However, the source term, $\frac{\partial H}{\partial t}$, can also be estimated at the current time step in which the DOC, $\alpha_t = \alpha(t)$, has to be solved iteratively with temperature in a coupled manner. A hybrid scheme is used, in which the convective term in Eq. (12) is evaluated at the previous time step as:

$$\rho_c C_{p,c}\left[\frac{\partial T}{\partial t}\right]^{k+1} = \left[\nabla(k_c \nabla T)\right]^{k+1} + \left[\frac{\partial H}{\partial t}\right]^{k+1} - \rho_c C_{p,c}\left[\frac{\partial(v_z T)}{\partial z}\right]^k \tag{12}$$

where

$$\left[\frac{dH}{dt}\right]^{k+1} = H_r\left[K_0 \exp\left(\frac{-\Delta E}{RT}\right)\left(1-\alpha_t^{k+1}\right) + \frac{\partial\left(v_z \alpha_t^{k+1}\right)}{\partial z}\right]^{k+1} \tag{13}$$

$$\alpha_t^{k+1} = 1 - \left[1 + (1-n)S^{k+1}\right]^{\frac{1}{1-n}} \tag{14}$$

$$S^{k+1} = S^k + K_0 \exp\left(\frac{-\Delta E}{RT^k}\right)\left(t^{k+1} - t^k\right) \tag{15}$$

3.2 Material shrinkage

During pultrusion, resin shrinks as it cures and the foam as well as the curing composites expand due to the rise in temperature. A unit dimensional change for control volume *j*, δ^j, is calculated as the function of appropriate thermal expansion and volumetric shrinkage for the resin as:

$$\delta_r^j = \left(1 - \frac{\gamma_r \alpha_T^j}{100}\right)^{1/3} \left[1 + \vartheta_r\left(T_T^j - T_o^j\right)\right] \tag{16}$$

where ϑ_r is the thermal expansion coefficient and γ the percentage volumetric shrinkage, which are set in this study as 4.5e-5 (1/^{o}C) and 4% respectively for the resin. The terms T_T^j and α_t^j refer to the CV temperature and DOC respectively with the convective effects, that arise from the flow of thermal energy and resin mass from one CV to another, added in. When a volume of composites ΔV^j, moves from control volume $j-1$ to control volume j, separated by a distance L_j over a small time increment Δt, the change in CV temperature ΔT^j can be obtained as:

$$\Delta T^j = \frac{v_z \Delta t}{L^j}\left(\frac{\rho_c^{j-1} C_{pc}^{j-1}}{\rho_c^j C_{pc}^j} T^{j-1} - T^j\right) \tag{17}$$

The ΔT^j is added to T^j to obtain T_T^j. In the same way, the change in α for control volume j, $\Delta\alpha^j$, can be calculated as:

$$\Delta\alpha^j = \frac{v_z \Delta t^j}{L^j}(\alpha^{j-1} - \alpha^j) \tag{18}$$

The sum of $\Delta\alpha^j$ and α^j gives the DOC of control volume j, α_t^j.

It may be noted that the FE/NCV procedure simulates the heat and mass transfer in a semi-steady manner. To keep it numerically stable, a number expressed as $CFL = \left|\frac{v_z \Delta t}{\Delta z}\right|$ should be less than 1.

Also, the convective term for temperature and degree of cure is treated as the first-order upwind scheme, in which the unwanted wiggles solutions due to larger Peclet number can be avoided [22]. Using β as relaxation factor an under-relaxation method is employed to update the DOC.

$$\alpha_t = \beta\alpha^{k+1} + (1-\beta)\alpha^k \tag{19}$$

In this study, the convergence limits of temperature and DOC were set at 0.0015^{o}C and 0.01% respectively and β=0.6 is used for revising DOC.

The above schemes provide inter-transferable ability between FEs and NCVs for both uncoupled and coupled heat transfer with exothermic reaction. Also, the energy conservation is established at every stage.

Further, the dimensional change in the foam, which is solid and non-reactive, is accounted for using:

$$\delta_r^j = \left[1 + \vartheta_{fo}\left(T_T^j - T_o^j\right)\right] \tag{20}$$

Finally, the output from Eqs. (16) and (20) will provide a relative dimensional change between the foam core and its GFRP face-sheets.

3.3 Effective material properties

Applying the rule of mixture based on volume fractions, the density of the composites in control volume *j* is calculated as:

$$\rho_c^j = \phi_r \left[\frac{\rho_r}{\left(\delta_r^j\right)^2} \right] + \phi_f \rho_f \tag{21}$$

The thermal properties of composites contained in control volume *j* are calculated after every time step using the rules of mixture based on final DOC and mass fractions (*m*) as [9]:

$$C_r^j = m_r \left[\alpha_T^j C_{pr}^s + \left(1 - \alpha_T^j\right) C_{pr}^u \right] + m_f C_{pf}^j \tag{22}$$

$$\frac{1}{\overline{k}_c^j} = \frac{m_f}{\overline{k}_f} + \frac{m_r}{\left[\left(1-\alpha_T^j\right)k_r^u + \alpha_T^j k_r^s\right]} \tag{23}$$

where $m_f = v_f \left(\frac{\rho_f}{\rho_c} \right)$, $m_r = 1 - m_f$ and superscripts *u* and *s* represent uncured and fully cured resin respectively.

3.4 Properties equivalence

It may be noted that the properties calculated using Eqs. (9) to (23) are required to be transferred accurately from NCVs to FEs and vice versa, at least once in one iteration. The volume

averaging technique based on volumes of the contributing sub-CVs was used for this purpose. Depending upon the contributions of each FE to the corresponding CV, the respective material properties are suitably converted to either FE or NCV properties using the volume-averaging. As seen in Fig. 2, the interface CVs consists of both, the foam and the GFRP and required a special dealing. The DOC and the related properties for such CVs are calculated and worked out based on resin content of each sub-CV. In general, if the foam is too dense to be considered porous, no resin would seep into it and the DOC = 0. Porous foam, depending upon the permeability (K_y) it offers, may allow some resin as its viscosity (η) lowers with temperature, at the interface from the face-sheets under certain pressure. The resin content in a sub-CV may then be calculated using 1D Darcy's law as:

$$Q^j = \sum_{0}^{k+1} S^j \left(\frac{P_{die} - P_{resin}}{L_{ij}} \right) \frac{K_y \Delta t}{\left(\eta_\infty e^{(\frac{U}{RT^j} + \kappa \alpha^j)} \right)} \tag{24}$$

where S^j is the contact area between foam and GFRP, and, the η_∞, U, κ are the constants related to resin determined by experiments. Once the resin content is known, it is merged into the overall resin content for the parent NCV, of which DOC is calculated similar to other NCVs. The rest of the analytical treatment for the interface CVs remains the same.

4. Case studies

In order to demonstrate the application of the developed FE/NCV simulation procedure, pultrusion process for a fairly large GFRP/foam sandwich panels was investigated. The die-composite assembly, however, was scale-down 6:1 such that the sandwich panel measured

400mm in width and 600 mm in length. It typically consisted of 36 mm thick foam as the core with 2 mm thick GFRP face sheets on both sides. The die consisted of 30 mm thick chrome steel all around. Only a quarter of the assembly was modeled employing symmetric conditions. A total of 4356 nodes with 3000, 8-noded, solid field elements were used to discretize the die-composites assembly. The cross-section was detailed, as in Fig. 2, using 36 nodes forming 25 solid field elements. Among these, finite elements 1 to 9 denoted the die, elements 10 to 17 defined the composite skin, and elements 18 to 25 formed the foam within the model. In order to facilitate the pultrusion of the sandwich panel through the die, the size of all finite elements in the pulling direction was maintained at 5 mm. A total of three heaters were mounted on the top surface of the heating die and three at the bottom in an arrangement as shown in Fig. 1. An appropriate part of only three heaters at the die top were considered for simulation purposes where the power supply for heating was maintained at 0.3 W/mm^2. The thermal properties of the materials and kinetic parameters for the polymer matrix used are respectively given in Tables 1(a) and 1(b). The infusion of foam with resin was assumed negligible in want of the porosity data. A number of case studies were conducted to investigate and underline the effect of various parameters as below.

4.1 Number of iterations

Due to the continuous nature of pultrusion process, the analysis was performed using evolution techniques [6] to achieve the steady state values of the processing parameters. It may be noted that the developed FE/NCV procedure allows pultrudate to move within the die by one element length (5mm in this case) in single iteration. Thus, it would take 120 iterations for the composites to move from one end of the 600mm-long die to the other end. Initially, when the heaters are just

switched on and temperature within the die is building up, the heat transfer remains unsteady. Eventually, as the number of iterations increase, the temperatures and the DOC profiles stabilize. Fig. 3 shows the predicted unsteady (80 iterations) and steady (1200 iterations) temperature distributions for the modeled die-composites assembly. Fig. 4 shows the DOC and temperature results obtained from different count of iterations ranging from 200 to 1200. As seen in Fig. 4(a), similar temperature profiles for the composites are obtained beyond 800 iterations. However, the stabilized DOC profile was achieved after 600 iterations with little fluctuation (the standard deviation of DOC at exit is less than 1%), Therefore, a total of 800 iterations were used for all subsequent simulation studies. Note that, in general, for a successful pultrusion of a part, its mean DOC at the die exit should be at least equal to 0.9 and above.

4.2 Heat transfer within foam

Since the materials used for the sandwich pultrudate, the GFRP and the foam, have different heat transfer and thermal expansion characteristics, it is important to examine the impact of these on the process as whole. In this section, thickness effects of the foam are reported. Three sizes of foam core - 12mm, 18 mm and 24 mm in thickness - were studied. The rest of details, especially the thickness of the GFRP face sheet and the die, were unchanged at 2mm and 30mm respectively. Fig. 5(a) and 5(b) show the plots of temperature measured along the loci of points beginning with node 10018 (i.e. the centerline of the GFRP layer) and with node 10003 (i.e. at the symmetry plane XZ for the foam), both parallel to the die length; see Fig. 1(a). The temperature distributions at the GFRP layer increased and at the foam symmetry plane decreased as thickness of the foam increased. As a result, relatively fast cure of the GFRP was achieved with the thicker foam due to the increased restriction on any transfer of heat energy off

the face-sheet due to relatively poor thermal conductivity of the adjacent foam; refer Fig. 6(c). However, the thickness effect was not conspicuous in this case, as both, the FRP and the foam, have low thermal conductivity.

4.3 Pull speed

Pull speed is the most important variable that has effect on the temperature profiles and thus the exit DOC of the pultruded part. As seen in Fig. 6(a), the centerline temperature experienced a drop as the pulling speed increased from 5mm/s to 10mm/s. This was because less and less heat transferred to the composites with the increase in the pull speed due to the shorter die resident time for the thermosetting material. Therefore, high DOC at the die exit was obtained when the minimum pull speed of 5mm/s was used; refer Fig. 6(b). It is also observed the DOC of the part at the die exit was less than 90% when the pulling speed was higher than 10mm/s. However, rapid curing of the part in the front section of the die is undesirable as it may result in poor consolidation, and cause cracks and defects in the pultrudate.

4.4 Die Heating

The pultrusion process operates under a very critical heat balance due to the exothermic nature of the reaction, the convective heat removal mechanism, and the ability to control temperatures only at the specific locations along the length of the die. Several researchers in the past have validated the thermo-chemical process models for the temperature profile of the part and the die for pultrusion of composites. Most of these studies have reported a good comparison of the steady state temperature profiles [6-8]. The effects of various set temperature for the 3 heating zones are investigated. Three different profiles such as (1) 170°C-150°C-150°C, (2) 150°C-

150°C-170°C and (3) 150°C-170°C-150°C, are studied. Note that the temperatures correspond to the front, middle, and rear die heaters, respectively.

The case (1) analysis shows that having a high set-temperature for the front heater is unacceptable because the centerline DOC of the reaches the maximum value of 1 at the early stage near the location of the front heater, as seen in Fig. 7(b). Such early curing will cause uneven stress induced within the composite skin between regions of fully cured and curing areas and thus defects induced by stress. It is also observed that there is no obvious difference between case (2) and (3). This could be due to the close temperature distribution among the front and middle heater between case (2) and (3), as shown in Fig. 7(a). However, the pattern of temperature arrangement from low to high is recommend due to the requirement of maximum DOC of the part at the exit of die. Accordingly, heater profiles are adjusted in order to optimize the effect.

4.5 Die thickness

Undoubtedly, the thickness of die or foam has an effect on the heat transfer and thus on DOC of the part. Three different dies with 10 mm, 30 mm and 50 mm thickness were modeled. From Fig. 8(a), it may be seen that the highest temperature was obtained for the 10 mm thick die, which caused the pultrudate to cure at a very earlier stage. It is also observed that irrespective of the die thickness, the product cured sufficiently (DOC < 0.9) before it left the die; refer Fig. 8(b). Thus, the 10 mm thick die was unsuitable whereas a 50 mm thick die would be heavy and unnecessary.

4.6 Material Shrinkage

When the shrinkage or thermal expansion of the GFRP occurs at a different rate with respect to the foam, an irregular-shaped pultrudate will be formed. Such irregularities are to be avoided as these parts are more prone to failure. The current FE\NCV formulation provides real-time quantitative analysis of the shape change for the pultrudate. As a demonstration case, a sandwich panel with 8 mm GFRP face-sheet and 24 mm foam was analyzed. In the initial stages, notable dimensional changes in the GFRP layer were observed. A maximum of 1.27 μm reduction in the thickness and 110 μm increase in the width of the face-sheet occurred while the die was just heating up. This was primarily due to higher rate of temperature rise near the die surface in contact with the heaters. After about 252 s (4.2 min), when the die temperature stabilized, the face-sheet thickness reduced further by 2.4 μm (3.67-1.27) while the expansion in the width dropped to zero due to little temperature difference between the die and the composites.

5. Conclusions

The presented case studies show that the developed FE /NCV procedure can be employed in a stepwise progressing simulation without losing numerical stability, robustness and reliability. The decoupled as well as coupled numerical schemes developed to cater for the effects of convective heat transfer and curing of a thermosetting matrix were compatible with the FE/NCV concept. The developed procedure was successfully implemented in 3D simulation for capturing time-variant dimensional and DOC details in multi-material thermal pultrusion, especially of GFRP/foam sandwich panels.

References

[1] Sumerak JE, The pultrusion process for automated manufacture of engineered composite profiles, Chapter 11 in: P.K. Mallick (Ed.), Composites Engineering Handbook, Marcel Dekker Inc., 549–577, 1997.

[2] Advani SG and Sozer EM, Process Modeling in Composites Manufacturing, Marcel Dekker Inc., USA 2003; 146–151.

[3] Valliappan M, Roux JA, Vaughan JG and Arafat ES, Die and post-die temperature and cure in graphite/ epoxy composites, Composites Part B, 1996; 27B(1): 1-9.

[4] Viola G, Portwood T, Ubrich P, DeGroot HR, Numerical optimization of pultrusion line operating parameters. 35th International SAMPE Symposium 1990; 1: 1968-1975.

[5] Wilcox JAD and Wright DT, Towards pultrusion process optimization using artificial neural networks. Journal of Materials Processing Technology 1998; 83(1-3): 131-141.

[6] Chachad, YR, Roux JA, Vaughan JG, Three-dimensional characterization of pultruded fiberglass-epoxy composite materials, Journal of Reinforced Plastics and Composites 1995; 14: 495-512

[7] Suratno BR, Ye L and Mai YW, Simulation of temperature and curing profiles in pultruded composite rods, Comp. Sci. Tech. 1998; 58: 192–197.

[8] Liu XL, Crouch IG and Lam YC, Simulation of heat transfer and cure in pultrusion with a general-purpose finite element package, Comp. Sci. Tech. 2000; 60: 857–864

[9] Joshi SC and Lam YC, Three-dimensional FE/NCV simulation of pultrusion process with temperature-dependent material properties including resin shrinkage, Comp. Sci. Tech. 2001; 61: 1539–1547.

[10] Joshi SC, Lam YC and Tun UW, Improved cure optimization in pultrusion with pre-heating and die-cooler temperature, Composites: Part A 2003; 12 (3): 1151–1159.

[11] Li SJ, Xu LQ, Ding ZM and Lee LJ, Experimental and theoretical analysis of pulling force in pultrusion and resin injection pultrusion(RIP)-Part II: Molding and Simulation, J Comp. Mat., 2003, 37:195-216

[12] Carlone P, Palazzo GS, Pasquino R, Pultrusion manufacturing process development by computational modeling and Methods, Math. Comput. Modelling, 2006, 44: 701–709

[13] Carlone P., Palazzo G.S. and Pasquino R., Pultrusion manufacturing process development: Cure optimization by hybrid computational methods, Comput. & Math. with Appli., 2007, 53: 1464-1471.

[14] Haj-Ali R.M., Zureick A.H.,Kilic M.H. and Steffen R., Three-Dimensional Micromechanics-Based Constitutive Framework for Analysis of Pultruded Composite Structures, J Eng Mech 2001, 127: 653–660.

[15] Muliana AH, Haj-Ali R, A multi-scale framework for layered composites with thermo-rheologically complex behaviors, Int. J. Solids & Struct., 2008, 45 (10): 2937-2963.

[16] Batch GL, Macosko CW, Heat transfer and Cure in Pultrusion: Model and Experimental verification, AICHE Journal, 1993;39 (7): 1228-1241.

[17] Britnell DJ, Tucker N, Smith GF and Wong SSF, Bent-pultrusion-a new method for the manufacture of pultrudate with controlled variation in curvature, *J Mater. Processing Techno.* 2003, 138: 311–315.

[18] Alberto C, Rizzi E and Papa E, Experimental characterization and numerical simulations of a syntactic foam/glass-fibre composite sandwich, Comp. Sci. Tech., 2000, 60: 2169-2180.

[19] Ben G and Shoji A, Pultrusion techniques and evaluations of sandwich beam using phenolic foam composite, Adv. Comp. Mater., 2005, 14(3): 277-288.

[20] Kosar V and Gomzi Z, Thermal effects of cure reaction for an unsaturated polyester in cylindrical moulds, *Chem. Biochem. Eng. Q.* 2001**;**15 (3): 101–108.

[21] LUSAS 13.0, Theory and User's Manuals, FEA Limited, Surrey, UK (1998).

[22] Pittman JFT, finite elements for field problems, Chapter 6, Fundamentals of polymer processing, ed. Tucker CL (1986)

Table 1(a), Material properties used in pultrusion analysis

material	Density (kg/m^3)	Specific heat (J/kg.C)	Thermal conductivity (W/m.K)		
Steel die	7833	461	55		
Resin matrix	1082	1680	0.144		
Glass fibre reinforcement	2580	825	kx	ky	kz
			1.16	1.16	6.6
Foam core	50	930	0.02		

Table 1(b), Resin kinetic parameters used in cure analysis

Heat of reaction (J /kg)	Pre-exponential constant K (1/s)	Order of reaction n	Activation energy (J/mol)
274680	$1.87x10^8$	1.285	71688

List of figures

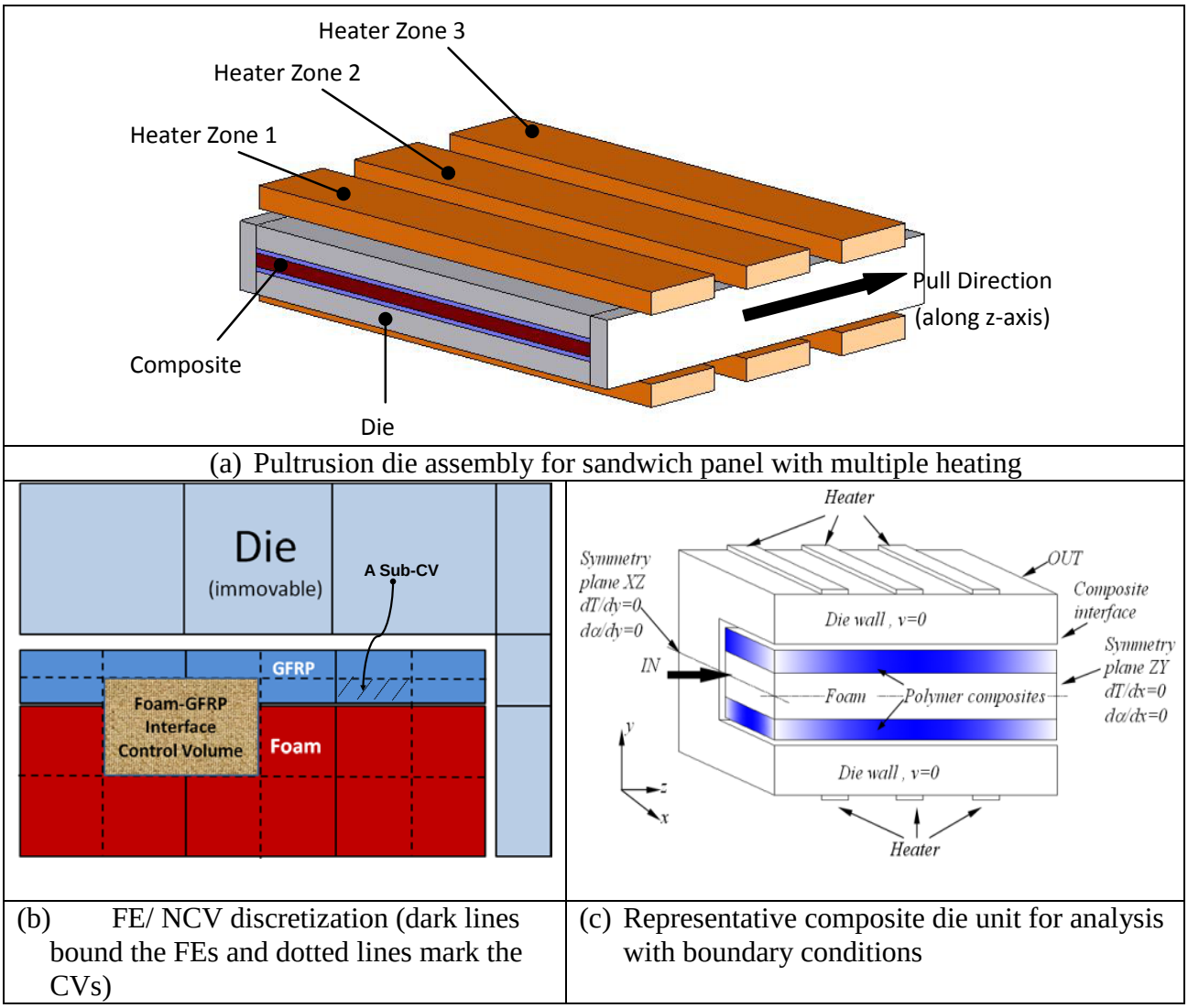

Figure 1 Geometric representation and FE/NCV discretization of pultrusion die-composites assembly

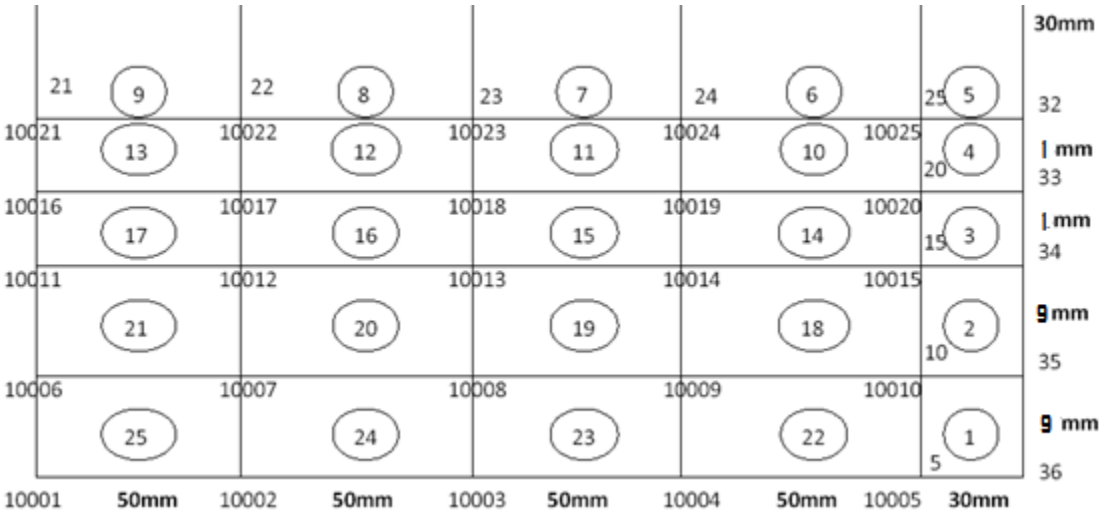

Figure 2 FE model of cross-section of a quarter pultrusion die assembly (not to scale) with foam sandwich pultrudate.

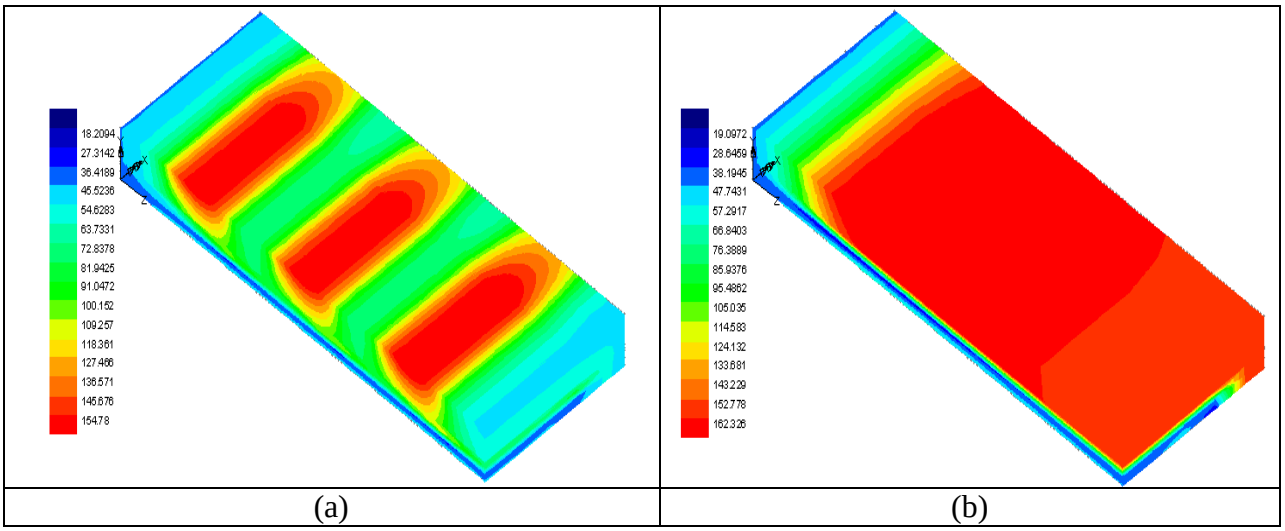

(a) (b)

Figure 3, Temperature distribution in modeled pultrusion die assembly at pulling speed of 5mm/s; (a) unsteady state (80 iterations),and (b) steady state (1200 iterations)

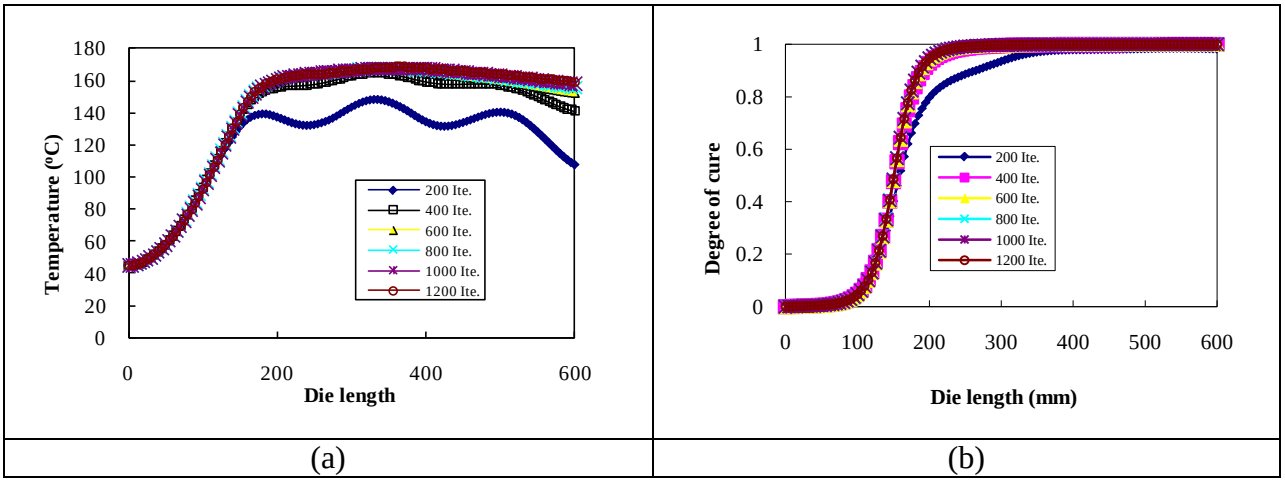

(a) (b)

Figure 4, (a) temperature and (b) degree of cure profiles along centerline (node 10018 in Fig. 2) of GFRP facesheet of sandwich pultrudate.

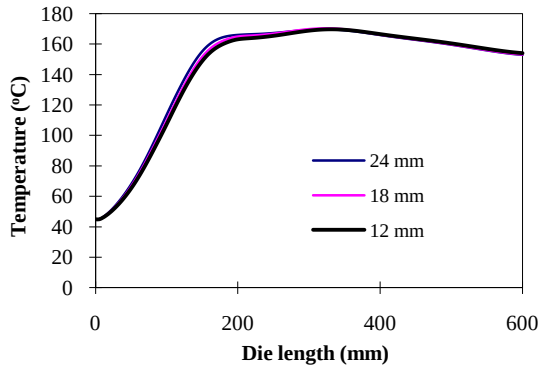

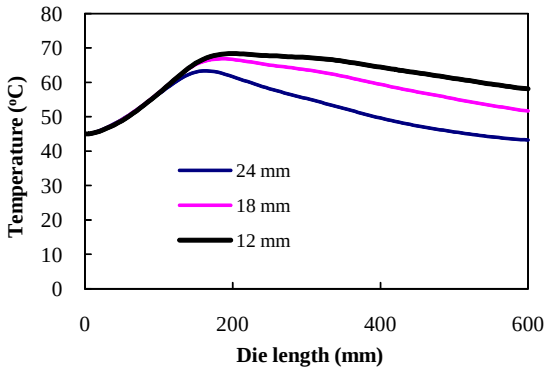

(a) (b)

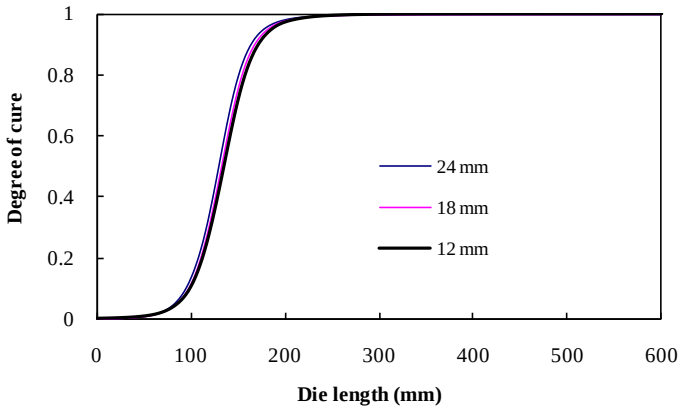

(c)

Figure 5, (a) temperature at node 10018 at the FRP mid-layer, (b) temperature at node 10003 at the symmetry plane XZ for the foam and (c) degree of cure at node 10018

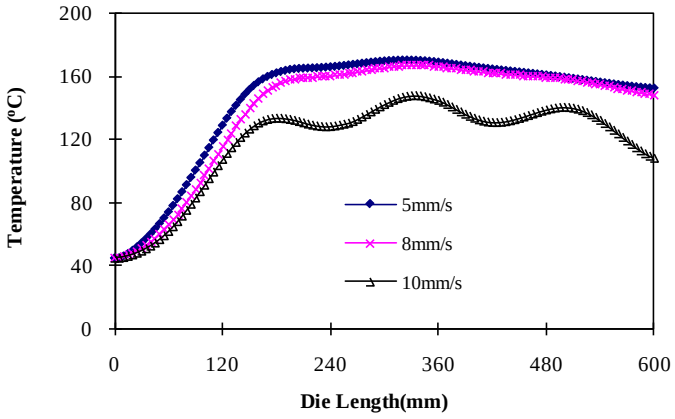

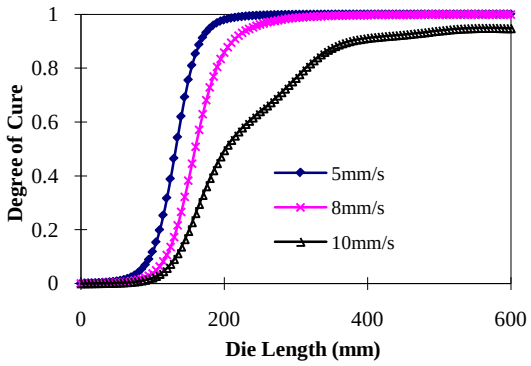

(a) (b)

Figure 6, (a) Plot of mean centerline temperature with different pulling speed and (b) DOC evolution profile at the centerline with different pulling speed along die length.

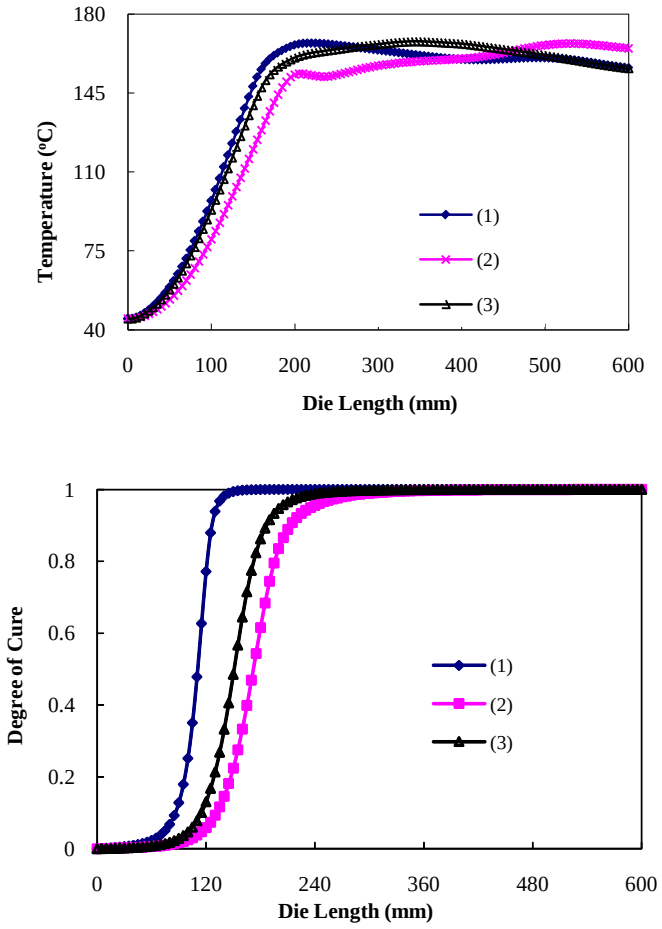

(a) (b)

Figure 7, (a) The temperature evolution profile at the centerline with different heater arrangement and (b) The DOC evolution profile at the centerline with different heater arrangement

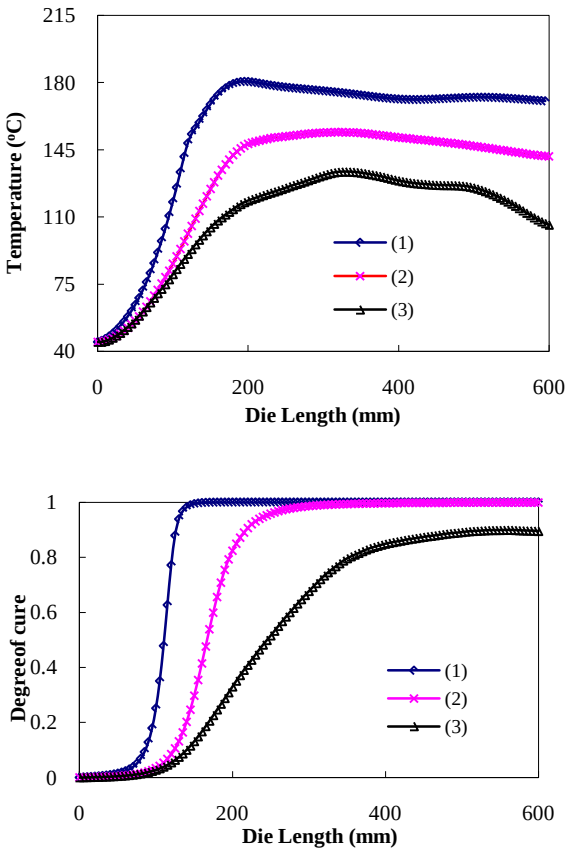

(a) (b)

Figure 8, (a) The temperature evolution profile at the centerline with different die thickness, and (b) The DOC evolution profile at the centerline with different die thickness